RSC Advances

PAPER

View Article Online
View Journal | View Issue



Cite this: *RSC Adv.*, 2020, **10**, 30150

# Improvement of mechanical properties of *in situ*-prepared HTPE binder in propellants

Keke Chen,[a] Xiaomu Wen,[a] Guoping Li,*[ab] Siping Pang [ab] and Yunjun Luo *[ab]

A new type of hydroxyl-terminal block copolymer (HTPE) binder with excellent mechanical properties was prepared using an *in situ* preparation method. Compared with traditional HTPE binder preparation, this method involves relatively simple operations, which not only reduces costs, but also does not require a complicated synthesis process to prepare the HTPE prepolymer intermediate. Thus, it is expected to replace the binder for HTPE propellants. The mechanical properties, crosslinking density, hydrogen bonding, and thermal performances of the prepared HTPE binders were investigated through tensile testing, low-field nuclear magnetic resonance (LF-NMR), Fourier-transform infrared spectroscopy (FTIR), and differential scanning calorimetry (DSC) analysis. The ultimate tensile strength ($\sigma_m$) of the *in situ*-prepared HTPE binder was 1.83 MPa, the fracture elongation ($\varepsilon_b$) was 371.61%, and the strength increased by 80% compared to the HTPE binders. The crosslink density ($V_e$) decreased with an increasing content of PEG and/or TDI. The proportion of H-bonds formed by the imino groups increased with the content of PEG and TDI and reached 81.49% at PEG and TDI contents of 50% and 80%, respectively, indicating a positive correlation between the H-bonds and $\sigma_m$. Based on the statistical theory of elasticity, the integrity of the curing networks showed that the contents of PEG and TDI affected the integrity of the curing networks. The DSC data of the *in situ*-prepared HTPE binder showed a lower glass transition temperature. Finally, compared to HTPE propellant, the strength and elongation of the *in situ*-prepared HTPE propellant increased by 206% and 135%, respectively. This exciting result greatly enhances the feasibility of the *in situ* HTPE preparation method.

Received 21st March 2020
Accepted 8th July 2020

DOI: 10.1039/d0ra02613a

rsc.li/rsc-advances



## 1. Introduction

Hydroxyl-terminal block copolymer (HTPE) was developed in the 1990s as an insensitive replacement of hydroxyl-terminated polybutadiene-based composite solid propellants. It has a less severe response in low vulnerability testing.[1–7] The HTPE prepolymer binder is typically synthesized by the active open-loop polymerization of polyethylene glycol (PEG) and polytetramethylene-ether-glycol (PTMG).[8,9] It is difficult to control the block structure in this complex synthesis route with a low yield. Therefore, novel polymerization methods have drawn much attention. Holmqvist[10,11] reported a polyethylene oxide–polytetrahydrofuran–polyethylene oxide (PEO–PTHF–PEO) triblock copolymer and compared it with polyethylene oxide/polypropylene oxide. Gerfried[12] used an acid catalyst to obtain polytetrahydrofuran and PEG block copolymer at high temperatures under an inert atmosphere. The molecular weight dispersion coefficient was 1.5–2.0. Neumer[13] produced a segmented copolymer of PTMEG and formaldehyde by an acidic-catalyzed condensation reaction of PTMEG and formaldehyde in a cyclohexylamine solution. However, this required extensive purification, including catalyst extraction and solvent drive-off. Luo[14] designed a new method to prepare a new kind of PTHF–PEO–PTHF HTPE. Macromolecular polyethylene glycol was the initiator in this method, and the boroethertrifluoride complex was the catalyst. Cationic open-loop polymerization of tetrahydrofuran occurred with a trace amount of epoxy propane, and the polytetrahydrofuran ether chain was bonded directly on both sides of the PEG. However, the uncertain molecular structure resulted in a molecular chain due to the epoxy propane. Hevus[15] used a commercial hydroxyl-terminated polytetrahydrofuran and polyethylene glycol producing polytetrahydrofuran/polyethylene glycol copolymer with multiple segments through coupled reactions of toluene diisocynate (TDI) and hydroxyl groups.

This work is dedicated to preparing a new type of hydroxyl-terminated block copolymer (HTPE) binder with excellent mechanical properties through an *in situ* preparation method. As the traditional HTPE propellant binder is composed of polytetrahydrofuran and polyethylene glycol multi-blocks, the low viscosity of PEG and PTMG with low molecular weights contributed to the mixing and pouring process of the composite solid propellants. In addition, due to the lack of soft segments,

[a]*School of Materials Science and Engineering, Beijing Institute of Technology, Beijing, 100081, China. E-mail: girlping3114@bit.edu.cn; yjluo@bit.edu.cn*

[b]*Key Laboratory for Ministry of Education of High Energy Density Materials, Beijing, 100081, China*

the strength of the HTPE propellant is insufficient, especially under high-temperature conditions. Due to the large difference in the reactivities of the NCO groups in TDI and (polyfunctional isocyanate) N100, it is possible to achieve a more reactive TDI to preferentially react with the –OH groups in the PEG/PTMG to achieve the effect of chain extension and ensure that the binders synthesized by this method have enough molecules to achieve good mechanical properties. Therefore, the binder made by this innovative *in situ* preparation method has more urethane groups, which could improve the strength of both the binder and propellant. Compared with the traditional HTPE binder preparation, this method involves a relatively simple operation process, which not only lowers costs but also does not require a complicated synthesis process to prepare the HTPE prepolymer intermediate. Thus, it is expected to replace the binder for HTPE propellants. The *in situ*-prepared HTPE binder was directly prepared by an *in situ* reaction of TDI and N100 in different proportions with PEG and PTMG.

Herein, low-molecular-weight PEG and PTMG were used as the mixed segments. TDI and N100 polyisocyanate were used as the chain extender and crosslinker to obtain a HTPE based polyurethane (PU). Soft and hard segment block structures were precisely controlled during polymerization, and the mechanical strength, thermal decomposition, and other properties of the prepared binders were systemically studied to analyze the correlation with the block structure. This reaction occurred under normal temperature and pressure and a neutral chemical environment without the addition of solvent. Moreover, HTPE-based propellants prepared with this innovative method have not yet been reported.

The excellent mechanical properties of the *in situ*-prepared HTPE binder will be the basis of new architectures, and these polymers have potential uses in propellant applications.

## 2. Experimental

### 2.1 Materials

The details of the chemical reagents in this work and their parameters are as follows. PEG with an average relative molecular mass $M_n \approx 200$ and average functionality of 2 was obtained from Xi Long Chemical Co., Ltd. PTMG was obtained from the Shanxi Province Chemical Research Institute with a number average molecular weight $M_n \approx 1000$ and average functionality of 2. HTPE[14] was self-prepared in our university lab with an average relative molecular mass $M_n \approx 4600$ and hydroxyl value of 32.26 mg KOH per g. High-purity (>99.5 vol%) toluene diisocyanate (TDI-80/20) with 2,4-TDI and 2,6-TDI contents of 80% and 20%, respectively, was obtained from Tianjin Guangfu Fine Chemical Research Institute. Polyfunctional isocyanate (N100) with a number-average molecular weight $M_n = 725$ and average functionality of 3.87 was obtained from the Liming Research Institute of Chemical Industry (Henan, China). Triphenyl bismuth (TPB) (purity of 99%) was obtained from Shanghai Institute of Organic Chemistry (Shanghai Municipality, China) and was formulated into a 0.5 wt% solution with dioctyl sebacate (DOS) as the solvent. Dibutyltin dilaurate (T12) from Shanghai Institute of Organic Chemistry (Shanghai Municipality, China) was formulated into a 0.5 wt% solution with dioctyl sebacate (DOS) as the solvent. Dioctyl sebacate (DOS) was analytically pure and obtained from Tianjin Guangfu Fine Chemical Research Institute. Bonding agent LBA-278, terminal cyano, and hydroxy-substituted polyamine was provided by Luoyang Liming Chemical Research Institute. Aluminum powder (Al), supplied by Jintian Aluminum Co., Ltd., had an average particle size of 6.8 μm. Fine grain ammonium perchlorate (AP), supplied by the Dalian Potassium Chlorate Plant, had an average particle size of 102 μm. Coarse grain ammonium perchlorate (AP), supplied by Dalian Potassium Chlorate Plant, had an average particle size of 300 μm,. Cyclotrimethylenetrinitramine (RDX), supplied by Jintian Aluminum Co., had an average particle size of 88 μm.

The PEG, PTMG, and HTPE binders mentioned above were vacuum dried at 60 °C for 9 h. Aluminum powder (Al), ammonium perchlorate (AP), and cyclotrimethylenetrinitramine (RDX) were dried in an oven at 60 °C for 7 d.

### 2.2 Preparation process

The main procedures for the preparation of the *in situ*-prepared HTPE binder are described as follows. Prepolymer PEG and PTMG1000 were first blended uniformly in a certain stoichiometric ratio followed by the addition of the curing agents TDI and N100 successively with 10 min of stirring for each. Finally, 0.3 wt% of the curing catalyst (the mass ratio of the TPB solution to the T12 solution was 3 : 1) was added with 10 min of stirring to achieve uniform mixing. The final mixture was further stirred and vacuumed at a temperature of 40 °C for 1 h to remove the air bubbles. It was then poured into a polytetrafluoroethylene matrix for casting into binder-shaped samples.

The main procedures for the preparation of the HTPE binder are described as follows. Prepolymer HTPE was first blended uniformly at a stoichiometric ratio followed by the addition of the crosslinker agent N100 with 10 min of stirring for each. Finally, 0.3 wt% of the curing catalyst (the mass ratio of the TPB solution to the T12 solution was 3 : 1) was added with 10 min of stirring to achieve uniform mixing. The final mixture was further stirred and vacuumed at a temperature of 40 °C for 1 h to remove the air bubbles. It was then poured into a polytetrafluoroethylene matrix for casting into binder-shaped samples.

The binders described above were placed in a desiccator for 24 h after curing in the incubator at 60 °C for 7 d. The sample preparation processes needed to be performed under ambient conditions with humidity values lower than 30% and a temperature around 25 °C. Moreover, the processing conditions, such as the stirring time, also must be well controlled. An HTPE binder was prepared using a procedure similar to that described above.

The PEG/PTMG and TDI/N100 ratios are important design parameters for obtaining chemical crosslinking in the *in situ*-prepared HTPE binders. In the prepared binder samples, the molar contents of PEG ($\chi$) were varied in the range of 20–80%, and the molar content of TDI ($\gamma$) was varied in the range of 20–80%. The $\chi$ and $\gamma$ values of the binder samples that were selected as curing parameters in this study are listed in Table 1.

Table 1 The formulation details of the binders and propellant compositions used in this study[a]

| *In situ*-prepared HTPE binders with different $\chi$ | | *In situ*-prepared HTPE binders with different $\gamma$ | | HTPE propellants | | |
|---|---|---|---|---|---|---|
| Symbol | $\chi$ | Symbol | $\gamma$ | Ingredients/ composition | *In situ*-prepared HTPE propellant | HTPE propellant |
| $S_{P20}$ | 20% | $S_{T20}$ | 20% | AL | 18% | 18% |
| $S_{P30}$ | 30% | $S_{T30}$ | 30% | Fine grain AP | 32% | 32% |
| $S_{P40}$ | 40% | $S_{T40}$ | 40% | Coarse grain AP | 20% | 20% |
| $S_{P50}$ | 50% | $S_{T50}$ | 50% | RDX | 10% | 10% |
| $S_{P60}$ | 60% | $S_{T60}$ | 60% | Bu-NENA | 10% | 10% |
| $S_{P70}$ | 70% | $S_{T70}$ | 70% | Binder | 9.5% | 9.5% |
| | | $S_{T80}$ | 80% | Bonding agent | 0.2% | 0.2% |
| | | | | Catalyst | 0.3% | 0.3% |

[a] $\chi$ represents the ratio of –OH in the PEG to the total –OH in the PEG and PTMG; $\gamma$ represents the ratio of –NCO in the TDI to the total NCO in the TDI and N100.

The sample preparation processes needed to be performed under ambient conditions with a humidity of less than 30% and a temperature of approximately 25 °C. Moreover, the processing conditions, such as the stirring time, also needed to be well controlled. Using a process similar to that described above, an HTPE binder was also prepared for comparison, denoted as $S_H$, whose $R$ value (the curing parameter $R$ denotes the equivalent ratio of isocyanate (–NCO) to hydroxyl (–OH) groups, $R = 1.2$) was consistent with the *in situ*-prepared HTPE binders. $\gamma$ represents the ratio of –NCO in the TDI to the total NCO in the TDI and N100.

PEG/PTMG and other liquid ingredients (except curative) were charged into a kneading mixer with a capacity of 5 L and mixed for 30 min. Next, aluminum powder was added in two steps. Ammonium perchlorate powder and RDX were added separately so that homogenous mixing could occur. The overall

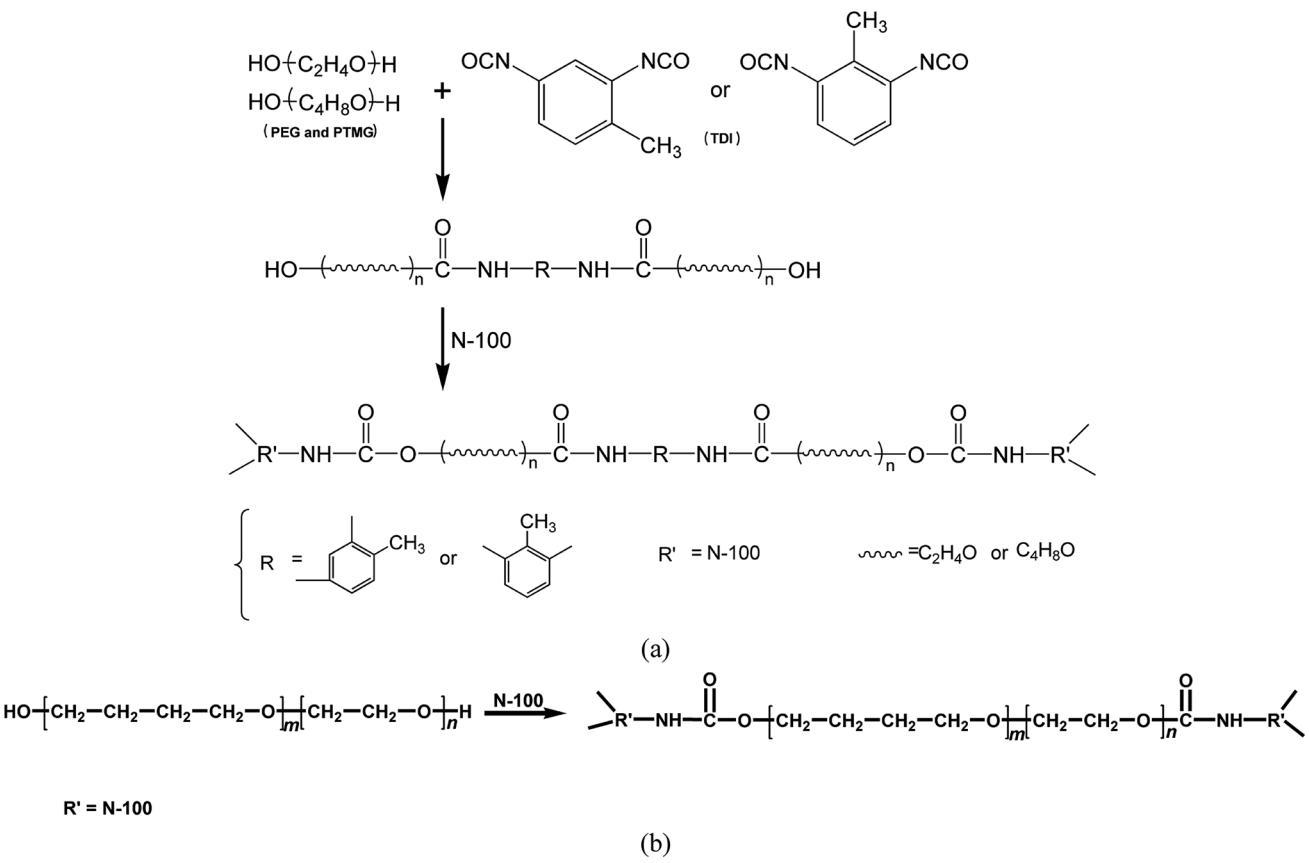


Fig. 1 Curing reaction for synthesizing the (a) *in situ*-prepared and (b) traditional HTPE binders.

 

mixing temperature was maintained at 50 °C. After the addition of all of the solid ingredients, the mixing was performed under a vacuum environment at 50 °C and −0.1 MPa and kneaded for 1.5 h at a kneading speed of 50 rpm. At this stage, TDI and N100 were added, and the mixture was further mixed for another 30 min followed by vacuum mixing for another 30 min to drive out entrapped air. Finally, a curing catalyst was added, and the mixture was kneaded for 1.5 h at a kneading speed of 50 rpm in a vacuum environment at 50–60 °C and −0.1 MPa. The mixture was cast into a mold and cured at 50 °C for 7 d, and the cured sample was used to evaluate its different properties. Using a process similar to that described above, a HTPE propellant was also prepared for comparison, whose $R$ value ($R = 1.2$) was consistent with the *in situ*-prepared HTPE propellant, but the binder was different.

The propellant samples contained 80% solid filler, 9.5% binder, 10% plasticizer, and 0.5% other materials. In addition, the binder for the *in situ*-prepared HTPE propellant was $S_{T80}$, and the binder for the HTPE propellant was $S_H$. The specific formulations of the *in situ*-prepared and HTPE propellants are given in Table 1.

### 2.3 Measurements

A WD-4005 AGS-J electronic universal testing machine (Shimadzu Corporation, GB/T 528-1998) was used to perform tensile tests using dumbbell-shaped samples at 25 °C with a strain rate of 100 mm $min^{-1}$. The crosslink density was examined with a VTMR20010V-T low-field NMR spectrometer provided by the Shanghai Newman Corporation. Fourier-transform infrared spectroscopy (FTIR) measurements were performed using a Nicolet 8700 from the Thermo Electron Corporation. These were performed with 48 scans in the middle infrared region with a spectral resolution of 2 $cm^{-1}$ and spectral range 4000–500 $cm^{-1}$. Binder samples with masses of 10 mg were placed in alumina pans and subjected to differential scanning calorimetry (DSC) analysis in a Setaram DSC131 under a nitrogen atmosphere at a flow rate of 40 mL $min^{-1}$ with a heating temperature range of −100 to 150 °C.

## 3. Results and discussion

### 3.1 Infrared spectrum

The binder plays a critical role in forming a three-dimensional network through chemical reactions. It provides combustible elements, such as carbon and hydrogen, in the combustion process and bonds with various filler components in the propellant to produce good mechanical properties. The binder generally must meet the following basic conditions: (1) the binder must be a liquid low-volatile prepolymer capable of withstanding the high vacuum during the mixing and casting of the slurry. (2) The binder must have good compatibility with other components in the propellant. (3) The binder must have a higher volume fraction of the solid filler, *i.e.*, a lower viscosity. (4) The binder must have good curing reaction capabilities, *i.e.*, the curing reaction can be carried out at a lower temperature (less than 60–70 °C), and the small molecule product must not be released in the reaction. The crosslinking reaction should be controllable such that the slurry has adequate fluidity during the mixing and casting and to ensure that the slurry has a sufficient pot life. (5) The binder must have a lower glass transition temperature.

The prepolymers PEG and PTMG used were low-volatility liquid polymers with low viscosities, low glass transition temperatures, and good curing reaction properties. These features satisfied the requirements of solid propellants for binders. In this experiment, PEG and PTMG were used as the mixed soft segment, and the chains were extended by the reaction of –NCO groups in TDI with –OH in the polyether soft segment so that PEG and PTMG were connected by TDI hard segments. The system formed a crosslinked network structure *via* N100 to combine the excellent properties of the two systems. The specific reaction principles are shown in Fig. 1a. The curing reaction for synthesizing the HTPE binder is shown in Fig. 1b.

To confirm that the *in situ*-prepared HTPE binder had formed, the structure of the prepared binder was characterized by FTIR, as shown in Fig. 2.

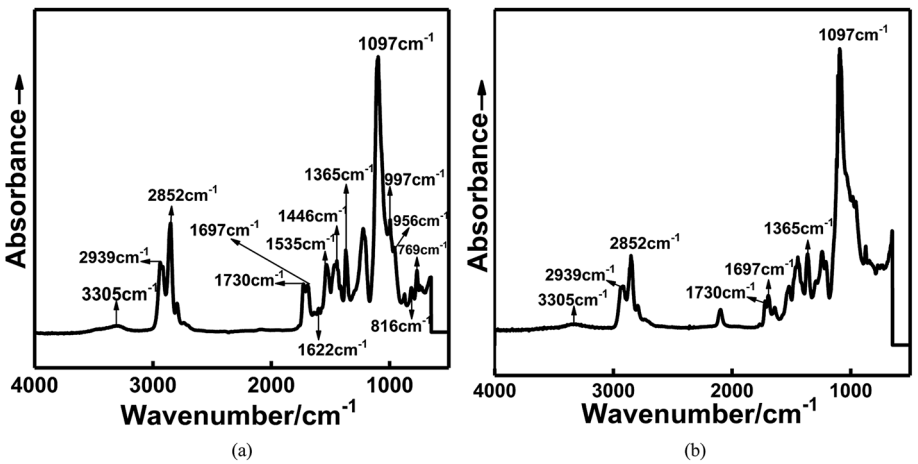


Fig. 2 FTIR curve of (a) *in situ*-prepared and (b) traditional HTPE binders.

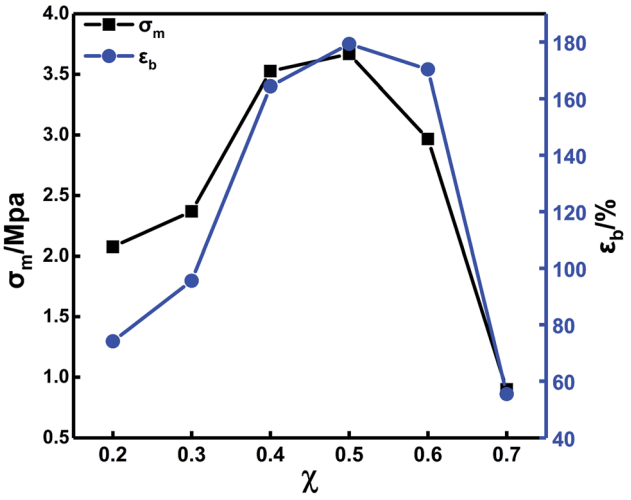


Fig. 3 Stress–strain curves of *in situ*-prepared HTPE binders with different $\chi$.

Fig. 2 shows the infrared spectra of the *in situ*-prepared HTPE and HTPE binders. The wide absorption band at 3305 $cm^{-1}$ is caused by valence vibrations of the associated amide NH groups. An amide band is found at 1535 $cm^{-1}$. A doublet of the absorption bands at 1097 $cm^{-1}$ appeared, indicating that the product molecular chain contained ether bonds (C–O–C), and methylene appeared at 2852 and 2939 $cm^{-1}$. The stretching vibration of amine (–NH) bond on urethane linkages appeared at 3345 $cm^{-1}$, and the stretching vibration of amide carbonyl (–C=O) bond appeared at 1730 $cm^{-1}$ and 1697 $cm^{-1}$, indicating the formation of new urethane groups. In addition, the presence of 2,4-tolylene and 2,6-tolylene moieties is confirmed by absorption bands at 769, 816, 956, and 997 $cm^{-1}$ (out-of-plane and in-plane deformation vibrations of aromatic C–H bonds, respectively), 1353 $cm^{-1}$ (symmetric stretching of methyl group in tolylene fragment), and 1446 and 1622 $cm^{-1}$ (vibrations of the aromatic ring). These analyses show that the HTPE-based polyurethane binders were successfully synthesized. The structures of the synthesized polymers are confirmed by FTIR.

In addition to the absence of the benzene ring structure, the main difference compared to the *in situ*-prepared HTPE binders were that the 2200 $cm^{-1}$ peak attributed to the isocyanate absorption appears in the infrared absorption spectrum of the HTPE binders. The main reason for this difference is that the molecular weight of the HTPE prepolymer (4000) is larger than that of the *in situ*-prepared HTPE binder (200–400), making the synthesis reactivity of the HTPE binders are lower than that of the *in situ*-prepared HTPE binders, so there exists residual curing agent in the HTPE binder.

### 3.2 Mechanical properties

The mechanical properties of the solid propellants are determined by the binder. The curing parameters play an important role in the mechanical properties of the binder. Both PEG and PTMG are hydroxyl (–OH)-terminated polyether, which can react with isocyanate (–NCO) to form carbamates. The difference is that the PEG has a smaller molecular weight and higher reactivity. The blending of these two has a greater impact on the mechanical properties and the crosslinking network structure. Therefore, it is important to study the blending ratio of PEG/PTMG and examine its effect on the mechanical properties of the binder. First, the binder file mechanical properties were investigated by changing the PEG/PTMG ratio with TDI/N100 = 1 and $R$ = 1.2 (the value of $R$ was used in all the subsequent analysis.).

Fig. 3 shows that the ultimate tensile strength ($\sigma_m$) and the fracture elongation ($\varepsilon_b$) increase with increasing PEG content. They reach maxima at a PEG content of 50%. Decreases in both $\sigma_m$ and $\varepsilon_b$ were detected with further increases in the PEG content. Compared to the PTMG, the PEG binder exhibits a small steric hindrance and a higher molecular chain activity because the PEG has a small molecular weight—this causes a higher reaction activity. Therefore, TDI preferentially extended the chain reaction with PEG in the blending system.

There are more hard segments of polyurethane elastomers with a fixed $R$ value and a high hydroxyl value due to the PEG content and greater amount of curing agent. Thus, $\sigma_m$ increases with increasing PEG content. The content of oxygen atoms in the segments of PEG is higher than that in the PTMG, and the flexibility of the chains is better. Therefore, $\varepsilon_b$ increases as the content of PEG increases. When the content of PEG continues to increase, the content of PTMG decreases accordingly leading to defects in the crosslinked network structure and a reduction in $\sigma_m$ and $\varepsilon_b$.

TDI is a difunctional curing agent and acts as a chain extender for PEG and PTMG. When N100 is the only polyfunctional component in the formulation, it functions as a crosslinking agent in the crosslinked network. Therefore, the change of the TDI/N100 ratio inevitably impact the crosslinking network structure in the propellant, affecting the mechanical properties.

Fig. 4 shows that with increasing TDI content, $\sigma_m$ first increases and then decreases. The $\varepsilon_b$ increases continuously. In

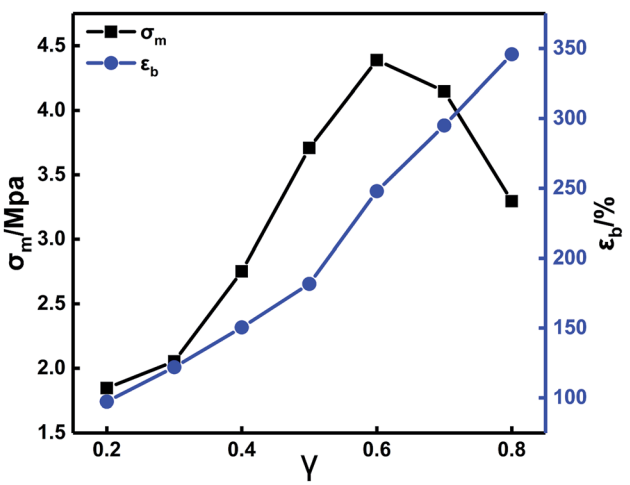


Fig. 4 Stress–strain curves of *in situ*-prepared HTPE binders with different $\gamma$.

the TDI/N100 mixture, TDI has a higher activity of isocyanate groups than the N100. Thus, TDI preferentially reacts with the hydroxyl groups in PEG and PTMG to form urethane groups, leading to longer molecular chains and higher elongation. In addition, since the TDI molecule contains a benzene ring, the content of urethane groups increases with increasing TDI content. This causes micro phase separation[16–18] and improvements in the mechanical properties. The further increase in the TDI content above a certain value (0.6) lead to a drastically reduced N100 content. Consequently, the density of crosslinking points and the $\sigma_m$ of the system were reduced. By optimizing the formulation parameters of the *in situ*-prepared HTPE binders, a sample with good comprehensive mechanical properties ($\sigma_m = 3.29$ MPa, $\varepsilon_b = 345.76\%$) was finally obtained.

In the present work, the corresponding values of $\sigma_m$ and $\varepsilon_b$ for the HTPE binder are 1.83 MPa and 371.61% respectively, when the curing parameter $R$ is held constant ($R = 1.2$). The $\sigma_m$ value of the *in situ*-prepared HTPE binder is 1.84 times that of the HTPE binders ($\sigma_m = 1.78$ MPa, $\varepsilon_b = 137.79\%$) achieved by Mao[19] and the $\varepsilon_b$ is 2.52 times greater. Similar values for the HTPE binders ($R = 1.2$) were obtained also by Wen[20] ($\sigma_m =$ 1.6 MPa and $\varepsilon_b = 150\%$). The $\sigma_m$ of the *in situ*-prepared HTPE binders is significantly better than that of the HTPE binders, indicating that the *in situ*-prepared HTPE has potential applications in the field of solid HTPE propellants.

According to the comparative analysis, the mechanical properties of the *in situ*-prepared HTPE binders were superior to those of the HTPE binders. There were evident differences in the main chain structures between the two kinds of HTPE binders. The PEG and PTMG segments in the *in situ*-prepared HTPE binders were connected by urethane bonds formed by the hydroxyl groups of PEG and PTMG and the isocyanate in TDI, but the PEG and PTMG segments in the HTPE binders were connected by ether bonds. Because the polarity of the urethane is greater than that of the ether, the *in situ*-prepared HTPE binders formed hydrogen bonds more easily than the HTPE binders, and micro phase separation occurs more easily. Therefore, the mechanical properties of the *in situ*-prepared HTPE binders were superior to those of the HTPE binders.

### 3.3 Crosslink density test

For thermosetting binders and propellants, crosslinked network structures are a direct factor and have a dominant effect on the mechanical properties.[21] LF-NMR is a common technique for studying the crosslinked network structure of polyurethane.[22] Thus, the crosslink density of the polyurethanes in this work were examined by LF-NMR. The chemical environment and the of restraint degree of the hydrogen atoms are different in the polymer, resulting in different lateral relaxation times ($T_2$) (*i.e.*, the time when the transverse magnetization vector decayed to 0). In NMR, proton transitions from a higher energy level to a lower energy level occur after the RF pulse is stopped. The relaxation mechanism of hydrogen atoms is sensitive to the movement of molecular chains. Therefore, the $T_2$ values of hydrogen atoms can be used to characterize the degree of movement and crosslinking of polymer chains. In previous work[23,24] a crosslink density (XLD) analysis was done using an XLD regression model, and this model is used herein to determine the crosslink density. The expression of the XLD model is as follows:

$$M(t) = A\exp\left(-\frac{t}{T_2} - \frac{qM_{rl}t^2}{2}\right) + A\exp\left(-\frac{t}{T_1}\right) + A_0, \quad (1)$$

where $M(t)$ is the amount of signal attenuation, $A$ and $B$ are the ratios of the signals corresponding to the crosslinked and tailing chain parts with respect to the signal of the entire polymer, respectively, $A_0$ is the DC (direct current) component of the signal without explicit physical significance, $T_2$ is the relaxation time of the crosslinked part of the signal, $T_1$ and $T_2$ represent the relaxation times of the signals corresponding to the hanging tail chain and the crosslink, respectively, $q$ is the anisotropy rate of the crosslinked part, and $M_{rl}$ is the residual dipole moment of the sample below the glassy temperature.

The crosslink density was obtained using the following equation after fitting each parameter using eqn (1):

$$V_e = \frac{5\rho N\sqrt{qM_{rl}}}{3CM}, \quad (2)$$

where $\rho$ is the of the polymer density, $N$ is the number of bonds in the backbone of the repeating unit and, $C$ is the number of bonds in the main chain in the Kuhn segment, and $M$ represents the molar mass of the repeating unit. $T_2$ of the *in situ*-prepared HTPE binder was carefully examined with the XLD model for regression analysis. The crosslink density of each binder was calculated, as shown in Table 2. In addition, the LF-NMR was calibrated by the Q-FID sequence. After multiple debugging steps, the "hot tail" part of the $T_2$ attenuation curve is less than 1/3 under the condition that the sampling point number equals 1024 with a sampling frequency SW = 200. The signal recovery time to balance TW is 1000, and the number of echoes (NECH) is 12 000. For 1024 points, the result is plotted in Fig. 3, which indicated that the selected parameters are reasonable.

Table 2 Curing network parameters of *in situ*-prepared HTPE binders with different $\chi$ and $\gamma$, the HTPE binder ($S_H$)

| Samples | $T_2$/ms | $V_e \times 10^{-4}$/mol cm$^{-3}$ | $M_c$/g mol$^{-1}$ |
|---|---|---|---|
| $S_{p20}$ | 6.37 | 3.45 | 2900 |
| $S_{p30}$ | 5.33 | 3.48 | 2873 |
| $S_{p40}$ | 4.62 | 5.30 | 1890 |
| $S_{p50}$ | 3.94 | 5.85 | 1750 |
| $S_{p60}$ | 2.78 | 5.77 | 1730 |
| $S_{p70}$ | 1.61 | 6.03 | 1660 |
| $S_{T20}$ | 5.09 | 5.85 | 1710 |
| $S_{T30}$ | 4.92 | 5.70 | 1730 |
| $S_{T40}$ | 4.06 | 5.66 | 1770 |
| $S_{T50}$ | 3.94 | 5.70 | 1750 |
| $S_{T60}$ | 3.62 | 5.25 | 1900 |
| $S_{T70}$ | 3.50 | 5.37 | 1860 |
| $S_{T80}$ | 3.89 | 5.33 | 1880 |
| $S_H$ | 3.46 | 5.07 | 1.97 |

According to Table 2, increasing the PEG content leads to an overall decrease in the $T_2$ value of the binder. This is mainly because the increase in the PEG content in the system can increase the hard segment content, which forms more crosslinking points. More junctions will provide a stronger binding effect of the segment. Moreover, the overall $T_2$ decreases with increasing PEG content because $T_2$ is related to the movement ability of the molecular chain. The crosslinking density ($V_e$) increases continuously with increasing $\chi$. This is because PEG has a small molecular weight but a large hydroxyl value and a large number of hydroxyl groups, which requires an increase amount of TDI/N100. However, the molecular weight between crosslinks ($M_c$) show the opposite variation with respect to $V_e$. The decrease in $M_c$ weakens the molecular chain's ability.

Similar to PEG, the increase in $\gamma$ also leads to a general decreasing trend of $T_2$, which is related to the molecular chain's movement ability. As $\gamma$ increases in the system, more TDI hard segments are mixed into the soft segment. The presence of the benzene rings in the TDI cause the segments to experience a stronger binding effect. Table 2 shows that TDI has the opposite effect on $V_e$ to that of PEG, *i.e.*, $V_e$ decreases with increasing TDI. The reason for the decrease by the TDI is that the corresponding N100 polyfunctional isocyanate content decreases with increasing TDI, leading to a lower potential for the formation of crosslinking points. *In situ* preparation of the HTPE binder yielded a slightly higher crosslink density than that of the HTPE binder, because the molecular weights of PEG and PTMG is much smaller than that of the HTPE prepolymer.

### 3.4 Hydrogen bonding

The crosslinked network structure of the polyurethane binder contains not only the chemical crosslinking but also many physical crosslinks, including the entanglement of segments, hydrogen bonding between polar groups, and other interactions. Of these, hydrogen bonding can make the network structure of the polyurethane binder denser and improve the mechanical properties of the binders. For the *in situ*-prepared HTPE binders, H-bonds are formed either by the carbonyl (C=O) and imino (–NH–) groups on the carbamate or by the ether (–O–) and imino (–NH–) groups. Generally, the infrared absorption spectra of the carbonyl groups might be shifted toward a lower frequency upon the formation of the hydrogen bonding.[25] A stronger hydrogen bonding leads to a larger shift in the absorption spectrum.

Fig. 5 shows the FTIR spectra of the carbonyl groups in the *in situ*-prepared HTPE binders and the HTPE binder ($S_H$). The central wavenumber of the spectral absorption peak of the carbonyl groups is generally located in the region of 1695–1735 $cm^{-1}$. Fig. 5 shows that the carbonyl absorption peak of the urethane group is clearly divided into two parts, which indicates that the spectral peak has undergone a significant frequency shift after the hydrogen bond formed. Of these,

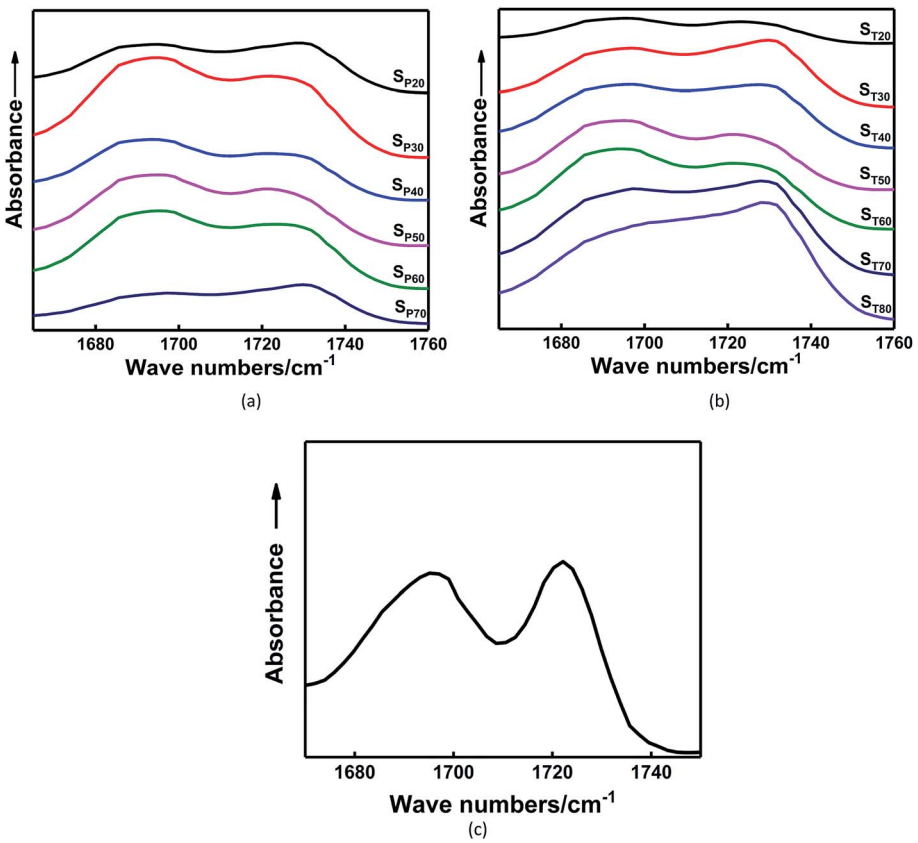


Fig. 5 Carbonyl region of the FTIR spectra for *in situ*-prepared HTPE binders with different (a) $\chi$ and (b) $\gamma$ and for the (c) HTPE binder.

 

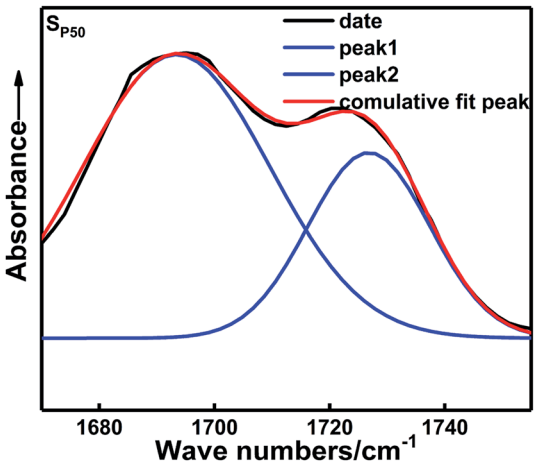


Fig. 6 Gaussian multi-peak fitting for the FTIR spectra of the carbonyl region.

Table 3 Peak area and percentage of H-bonded carbonyl groups in *in situ* prepared HTPE binders with different $\chi$ and $\gamma$, the HTPE binder ($S_H$)

| Samples | Area (1695 $cm^{-1}$) | Area (1721 $cm^{-1}$) | H-bonded carbonyl (%) |
|---|---|---|---|
| $S_{p20}$ | 12.90 | 6.18 | 67.59 |
| $S_{p30}$ | 22.70 | 10.88 | 67.60 |
| $S_{p40}$ | 14.29 | 6.78 | 67.82 |
| $S_{p50}$ | 15.83 | 7.20 | 68.73 |
| $S_{p60}$ | 18.35 | 8.60 | 68.09 |
| $S_{p70}$ | 8.74 | 4.17 | 67.70 |
| $S_{T20}$ | 5.70 | 2.77 | 67.30 |
| $S_{T30}$ | 16.36 | 7.80 | 67.72 |
| $S_{T40}$ | 17.36 | 8.07 | 68.27 |
| $S_{T50}$ | 15.83 | 7.20 | 68.73 |
| $S_{T60}$ | 19.43 | 8.61 | 69.29 |
| $S_{T70}$ | 26.03 | 10.61 | 71.04 |
| $S_{T80}$ | 38.12 | 8.66 | 81.47 |
| $S_H$ | 2.40 | 0.97 | 68.20 |

1725 $cm^{-1}$ is the absorption peak of the free carbonyl group, and 1695 $cm^{-1}$ is a hydrogen-bonded carbonyl absorption peak. However, the extent to which the different absorption peaks of H-bonded and free carbonyl groups overlapped make it difficult to analyze the distinctions. These overlapping bands were resolved through multi-peak Gaussian fitting to obtain the area and peak wavenumber of each peak. The detailed solution process and final results are shown in Fig. 6 and Table 3.

The areas of these peaks and their percentages are given in Table 3. Hydrogen bonding occurs within the *in situ*-prepared HTPE binders, and the central wavenumber of the carbonyl peak shifts from 1727 $cm^{-1}$ to approximately 1695 $cm^{-1}$, suggesting that most carbonyl groups contribute to the formation of H-bonds. Moreover, a rising trend in the percentage of H-bonded carbonyl groups occurs within the range $\chi$ = 20–50% because of the increasing concentration of carbamate (–NHCOO–) groups. The probability of bonding between the proton donating imino group (–NH–) and the carbonyl (C=O) or ether (–O–, on the PEG and PTMG backbone) groups also

Table 4 Curing network integrity of *in situ*-prepared HTPE binders with different $\chi$ and $\gamma$, and the HTPE binder

| Samples | $E$ (MPa) | $V_e$ ($10^{-4}$ mol $mL^{-1}$) | $M_c$ (g $mol^{-1}$) | $\rho$ (g $cm^{-3}$) | $D$ |
|---|---|---|---|---|---|
| $S_{p20}$ | 3.87 | 5.45 | 1840 | 1.024 | −0.4352 |
| $S_{p30}$ | 2.99 | 5.48 | 1830 | 1.024 | −0.1345 |
| $S_{p40}$ | 3.80 | 5.30 | 1890 | 1.024 | −0.0465 |
| $S_{p50}$ | 3.01 | 5.70 | 1750 | 1.024 | −0.4089 |
| $S_{p60}$ | 2.48 | 5.77 | 1730 | 1.024 | −0.6029 |
| $S_{p70}$ | 1.65 | 5.53 | 1810 | 1.024 | −0.8201 |
| $S_{T20}$ | 2.29 | 5.81 | 1720 | 1.024 | −0.6761 |
| $S_{T30}$ | 2.15 | 5.79 | 1730 | 1.024 | −0.7179 |
| $S_{T40}$ | 2.17 | 5.66 | 1770 | 1.024 | −0.6790 |
| $S_{T50}$ | 2.32 | 5.70 | 1750 | 1.024 | −0.6389 |
| $S_{T60}$ | 2.39 | 5.25 | 1900 | 1.024 | −0.5041 |
| $S_{T70}$ | 1.93 | 5.37 | 1860 | 1.024 | −0.6871 |
| $S_{T80}$ | 1.79 | 5.33 | 1880 | 1.024 | −0.7239 |
| $S_H$ | 1.58 | 5.07 | 1970 | 1.024 | −0.7303 |

increases. However, when $\chi$ increases from 50% to 70%, this interaction is reduced to 69.79%. The main reason for this is that the number of short and soft segments increases, and the regular structure of the soft segments is destroyed. The compatibility of the soft and hard segments is enhanced with a further increase in the PEG content. The soft segments make the distance between some hard segments, which is not conducive to the formation of hydrogen bonds and weakens the degree of hydrogen bonding.

Table 3 shows that the percentage of H-bonded carbonyl groups of the binder gradually increases with increasing $\gamma$. This is because the average molecular weights of the segments between the crosslinking points increases with increasing difunctional isocyanate content. More hard segments become embedded in the soft segments in the system, making it easier to form hydrogen bonds. The hydrogen bonding effect of the *in situ*-prepared HTPE binders and the HTPE binders are almost similar.

### 3.5 Integrity of curing networks

According to the statistical theory of the high elasticity of crosslinked structural rubber, all work done by the external forces on the system becomes the energy stored in the polyurethane binder, and the relationship between the shear modulus and the network structure parameters is as follows:

$$G = NkT = N'\rho kT/M_c = \rho RT/M_c, \quad (3)$$

where $N$ is the chain number in the curing network, $N_A$ is the Avogadro constant, $\rho$ is the density, and $R$ is the universal gas constant. Such an ideal network cannot be obtained in practice. There are other structural characteristics, which mainly include hydrogen bonding and defects such as entanglements, enclosed rings, pendant groups, and free chains. These structures cannot be accurately calculated with statistics. Thus, a correction factor $D$ can be introduced to express their contribution to the shear modulus:

$$G = (\rho RT/M_c) + D. \quad (4)$$

The correction factor $A$ represents the comprehensive contributions to the modulus of the interactions and defects. Using eqn (4) and the existing data, the correction factors ($D$) of polyurethane binders with different $\chi$ and $\gamma$ are calculated. The results are shown in Table 4.

The correction factors of the *in situ*-prepared HTPE binders are all negative values because the measured elastic moduli are higher than those computed, which indicates that the physical crosslinked structure formed by chain entanglement and hydrogen bonding in this system is not sufficient to offset the negative effects introduced by network defects (Table 4). This is mainly because the functional distribution of curing agent N100 is relatively wide. When some isocyanate molecules with higher functionality react with the polyether to form a network structure, a cyclic structure appears, which affects the integrity of the entire crosslinked network structure. With increasing $\chi$, the shear modulus correction factor $D$ increases first and then decreases. It reaches a maximum value when $\chi$ is 0.5. Therefore, the most complete curing network exists in the binder with a $\chi$ value of 0.5.

Table 4 aslo shows that as the TDI content increases, the shear modulus correction factor $D$ of the *in situ*-prepared HTPE binders increased continuously from −0.72 to −0.5 within the $\gamma$ range 0.2–0.6, because hydrogen bonding exhibits the same trend as the content of TDI range as compensated by the network structure defects. However, excess TDI in the binder enters the crosslinking network ($V_e$ decreases) and has negative effects on the network, even if there is a reduction in the relative content of carbamate and increased hydrogen bonding. Therefore, factor $D$ has the opposite trend within the PEG content ($\gamma$) range of 0.6–0.8. In addition, the shear modulus correction factor $D$ of the *in situ*-prepared HTPE binder is slightly higher than that of the HTPE binder, which shows that the structural integrity of the cross-linked network is better and it is more conducive to good mechanical properties. Although the correction factor remains negative, the relatively superior network which has the maximal, might be selected for application.

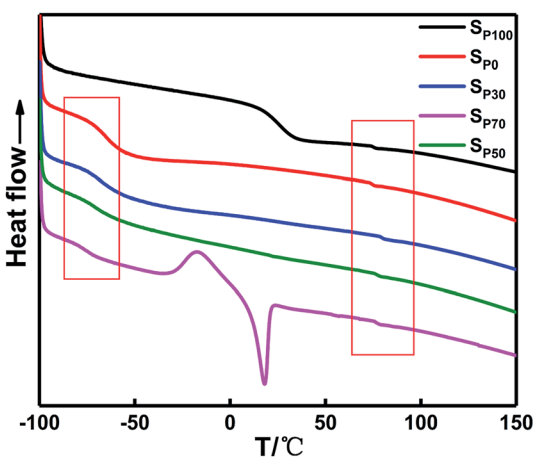


Fig. 7 DSC curves of *in situ*-prepared HTPE binders with different $\chi$.

### 3.6 DSC thermal performance

Weapons and equipment have a wide range of environmental adaptability to meet different application conditions, and the low temperature performance of solid propellants is particularly important. Relevant publications have reported that a glass transition temperature $T_g < -50$ °C is required for some large-scale, wall-mounted solid propellants. The low-temperature performance of propellants is mainly determined by the low-temperature performance of the binder. Therefore, the low-temperature performance of the binder is very important—especially the glass transition temperature. Therefore, in this section, the thermal performance of the *in situ*-prepared HTPE binder was studied and compared with that of the HTPE binder.

The polyurethane structure consists of a urethane hard segment and a polyether soft segment. At room temperature, the hard segment can provide a crosslinking point. Due to its lower glass transition temperature, the soft segment is in an amorphous state, which can provide elasticity to the material.[26,27] The glass transition temperature can be used to characterize the relative purities of the soft and hard segments, which reflects the degree of phase separation of these segments. The higher $T_g$ results in a greater content of the hard segment components in the soft segment phase with a greater degree of micro-phase separation. When the $T_g$ value is closer to the glass transition temperature of the pure soft segment, the smaller content of the hard segment component in the soft segment phase will be produced, and greater phase separation of the soft and hard segments occurs.

Fig. 7 and Table 5 show that the glass transition temperature ($T_g$) of the soft segments of the PEG binder ($S_{P100}$) is 25.5 °C, which is much greater than that of the soft segment in the PTMG binder ($S_{P0}$) with a value of −65.33 °C. The molecular weight of PEG is small, and the content of TDI required for curing and the rigidity of the molecular chain of the polyurethane increases, resulting in an increase in the $T_g$ of the *in situ*-prepared HTPE binders as $\chi$ increases. The $\Delta T_g$ value of the PTMG binder is the second smallest, which is closely related to the length of the chain. The *in situ*-prepared HTPE binders have

Table 5 $T_g$ data of *in situ* prepared HTPE binders and HTPE binders

| Samples | $T_{g,soft}$/°C | $T_{g,hard}$/°C | $\Delta T_g$/°C |
|---|---|---|---|
| $S_{p0}$ | −65.3 | 73.7 | 139.0 |
| $S_{p30}$ | −67.5 | 79.2 | 146.7 |
| $S_{p50}$ | −70.3 | 76.2 | 146.5 |
| $S_{p70}$ | −76.2 | 76.0 | 152.2 |
| $S_{p100}$ | 25.5 | 74.8 | 49.3 |
| $S_{T0}$ | −79.3 | 73.3 | 152.6 |
| $S_{T20}$ | −78.7 | 74.3 | 153.0 |
| $S_{T40}$ | −73.8 | 75.2 | 149.0 |
| $S_{T60}$ | −70.7 | 75.5 | 146.2 |
| $S_{T80}$ | −66.5 | 74.8 | 141.3 |
| $S_H$ | −74.2 | 72.7 | 146.9 |

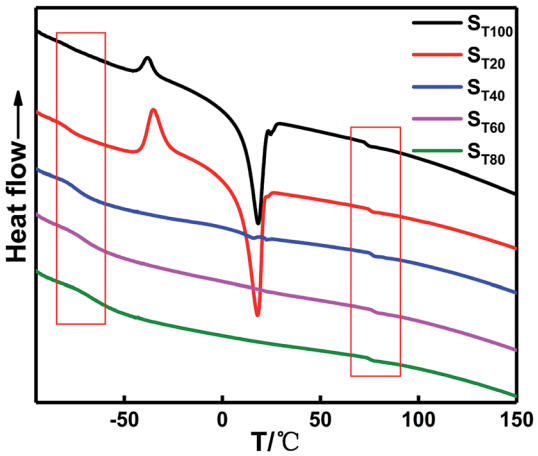


Fig. 8 DSC curve *in situ*-prepared HTPE binders with different $\gamma$.

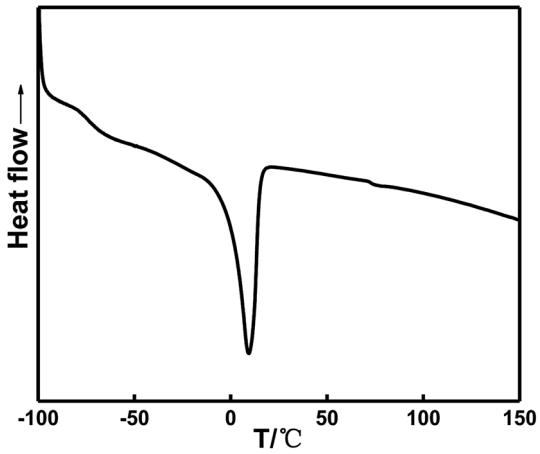


Fig. 9 DSC curve of the HTPE binder ($S_H$).

a glass transition temperature of the soft segment that gradually decreases with increasing PEG content ($\chi$). However, the melting peak of the PTMG occurs concurrently. With increasing PEG content ($\chi$), the degree of phase separation of the soft segment polyether increases in the system. The mechanical properties decrease at a greater rate. The $\Delta T_g$ value is smallest when $\chi$ is 0.5, indicating that the degree of mixing of the soft and hard segments is relatively large. The $T_g$ value is the largest when $\chi$ is 0.7, suggesting that the soft and hard segments are less mixed.

To study the effect of the TDI content on the thermodynamic behavior of the binder system, DSC tests were performed on binders with different $\gamma$ values. Table 5 shows the glass transition temperature data for different $\gamma$ values. The corresponding DSC and differential DSC curves are shown in Fig. 8.

Table 5 shows that the $T_g$ of the soft segment is −79.33 °C when the TDI is absent in the system, which is close to the melting temperature of the pure PEG component. The melting endotherm of the PTMG also appears in the system. When $\gamma$ is very small, the two polyether soft segments cannot be easily mixed only by relying on N100, and the phase separation degree of the soft segment polyether is greater. The melting endothermic peak of the system disappeared with increasing TDI content ($\gamma$). The soft segment polyether exhibited a single $T_g$, and the $T_g$ of the soft segment gradually increased, indicating that the phase mixing degree of the soft and hard segments increased. In addition, the PEG and PTMG units passed through the TDI chemical connections, which are better blended to form a uniform system. However, the $T_g$ of the hard segments changed slightly near 75 °C.

The endothermic peak in the system appears because the heating rate is higher than the cooling rate during the production of the sample, and the fraction of the free volume frozen in the glassy state when the melt is slowly cooled is small. Thus, the chain is not as heavy when the temperature is rapidly increased. Rows cannot quickly reach the equilibrium free volume fraction. The relaxation time of the segment rapidly decreases once the glass transition temperature is reached. The free volume suddenly increases to its equilibrium value. Thus, the DSC shows an endothermic peak.[28]

Fig. 9 and Table 5 show that the glass transition temperature of the soft segment in the HTPE binder is −74.17 °C, which is slightly lower than the glass transition temperature at −70.67 °C in the *in situ*-prepared HTPE binder. The similar values suggest that the *in situ*-prepared HTPE binder has a better degree of phase mixing and a lower glass transition temperature than the HTPE binder. Therefore, *in situ*-prepared HTPE binders are more viable than the HTPE binders based on the thermodynamics.

### 3.7 Application in propellant

From the analysis of the research results of these two binders, we can see that the mechanical properties of the *in situ*-prepared HTPE binder can reach those of the HTPE binder, and the tensile strength significantly improved. This laid the foundation for the application of *in situ*-prepared HTPE binder in propellants.

The new *in situ*-prepared HTPE propellant was prepared according to the procedure described in Section 2.2. It is compact and free of pores and cracks. The process performance was good—the propellant slurry had a low viscosity and good leveling properties.

The mechanical properties of the *in situ*-prepared HTPE propellant and HTPE propellant are given in Table 6. The mechanical properties of the *in situ*-prepared HTPE propellant are greatly improved. The strength increased by over 200% and the elongation increased by about 135% compared to the HTPE propellant.

Table 6 Propellant mechanical properties

| Sample | $\sigma_m$ (MPa) | $\varepsilon_b$ (%) |
|---|---|---|
| *In situ*-prepared HTPE propellant | 0.81 | 50.1 |
| HTPE propellant | 0.26 | 21.3 |

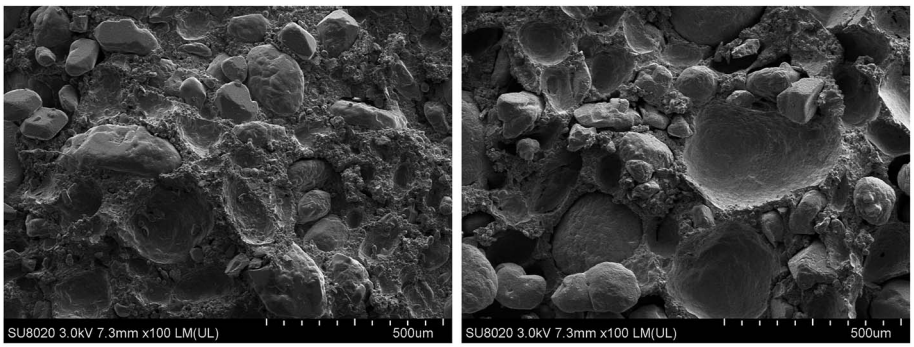


Fig. 10 (a) Microstructure surfaces of composite solid propellants use *in situ*-prepared HTPE (a) and HTPE (b) as binder.

To further study the differences between the mechanical properties of the two solid propellants, the microstructure surfaces of the *in situ*-prepared HTPE and the HTPE propellant specimens after tensile testing are shown in Fig. 10a and b, respectively. The HTPE propellant has a distinctly poor adhesion of the solid particle filler. More holes and bare particles are evident, indicating a greater amount of dewetting (Fig. 10b). The *in situ*-prepared HTPE propellant specimens did not form threads at the fracture surfaces after mechanical testing and seemed to have a significantly stronger binder–filler adhesion and fewer holes and bare particles, indicating that light dewetting occurred (Fig. 10a). The interactions of the bonding agent with the solid particle filler surfaces are presumably noncovalent by nature. This effect stems from the increase in the urethane bond density and the simultaneous increase in the cohesive energy density, which may have improved the adsorption of the binder on the polar surface of the filler particles. Thus, except for the mechanical properties of the *in situ*-prepared HTPE binder itself, adequate adhesion of the solid particles constituting the bulk of the composite material and the continuous binder matrix is critical for the good mechanical properties of the *in situ*-prepared HTPE propellant. This exciting result greatly enhances the feasibility of the proposed *in situ* preparation method and opens up a new realm for propellants.

## 4. Conclusions

We synthesized and characterized a novel *in situ*-prepared HTPE binder with PEG and PTMG functionalities. Uniaxial tensile tests were used to investigate their mechanical performances, and we concluded that the tensile strength of the *in situ*-prepared HTPE binder is significantly better than that of the HTPE binder. This indicates that the *in situ*-prepared HTPE has potential applications in the field of solid propellants *versus* HTPE.

The crosslinking density of the *in situ*-prepared HTPE binder exhibited a large range of variation, and it increased and decreased with increasing PEG and TDI contents, respectively. The proportion of hydrogen bonding varies with the content of PEG and TDI and can reach 81.50%. Based on the statistical theory of elasticity, the integrities of the curing networks were analyzed, showing that the content of PEG and TDI affected the integrity of the curing networks.

DSC analysis of the *in situ*-prepared HTPE binder shows a lower glass transition point of −70.67 °C, which can meet the application conditions for the solid propellants. Compared to the HTPE propellant, the mechanical properties of the *in situ*-prepared HTPE propellant are greatly improved. This will lead to new architectures, and these polymers have many potential uses as propellants.

## Conflicts of interest

The authors declare that they have no conflicts of interest.

## Acknowledgements

This work was funded by the Advanced Research Projects Agency (201920929091 and 40406010101).

## References

1 G. Lakrishnan, A. Linan and F. Williams, *J. Propul. Power*, 1992, **8**, 1167–1176.
2 J. R. Goleniewski and J. A. Roberts, *US Pat.*, 5348596, 1994.
3 J. Q. Li, X. Z. Fan, Q. F. Tang, J. Z. Li, G. Q. Wang, X. N. Ren and Z. T. Mei, *J. Solid Rocket Technol.*, 2019, **42**, 597–602.
4 D. Q. Yan, D. D. Xu and J. G. Shi, *J. Solid Rocket Technol.*, 2009, **32**, 644–649.
5 Q. F. Zhang and J. Q. Zhang, *J. Energ. Mater.*, 2004, **12**, 371–375.
6 K. H. Kim, C. K. Kim, J. C. Yoo and J. J. Yoh, *J. Propul. Power*, 2011, **27**, 822–827.
7 X. Yang, X. Q. Zhi, B. L. Yang and J. J. Li, *Chin. J. Explos. Propellants*, 2016, **39**, 84–89.
8 A. F. Zhang, H. Z. Zhang, H. C. Yang and X. D. Zhang, *Chin. Sci. Bull.*, 1990, **35**, 1881–1885.
9 J. R. Goleniewski and J. A. Roberts, *US Pat.* 5783769A, 1998.
10 G. Pruckmayr and R. B. Osborne, *US Pat.* 5284980A, 1994.
11 I. C. De Witte and E. J. Goethals, *Polym. Adv. Technol.*, 1999, **10**, 287–292.

 

12 G. Pruckmayr and R. B. Osborne, *US Pat.* 5284980A, 1994.
13 J. F. Neumer, *US Pat.* 5254744A, 1993.
14 C. D. Wang, Y. J. Luo, M. Xia, X. M. Li and K. Z. Mao, *J. Solid Rocket Technol.*, 2011, **34**, 202–206.
15 I. Hevus, A. Kohut and A. Voronov, *Macromolecules*, 2010, **43**, 7488–7494.
16 S. Velankar and S. L. Cooper, *Macromolecules*, 2000, **31**, 382–394.
17 S. J. Chen, Q. Cao, B. Jing, Y. L. Cai, P. S. Liu and J. L. Hu, *J. Appl. Polym. Sci.*, 2006, **102**, 5224–5231.
18 Sudaryanto, T. Nishino, S. Asaoka and K. Nakamae, *Int. J. Adhes. Adhes.*, 2001, **21**, 71–75.
19 K. Z. Mao, M. Xia and Y. J. Luo, *J. Elastomers Plast.*, 2016, **48**, 546–560.
20 X. M. Wen, G. P. Zhang, K. K. Chen, S. Yuan and Y. J. Luo, *Propellants, Explos., Pyrotech.*, 2020, **45**, 1–12.
21 Y. M. Ju, D. M. Kim and J. H. Lee, *Biomaterials*, 2000, **21**, 683–691.
22 H. G. Tattersall and G. Tappin, *J. Mater. Sci.*, 1966, **1**, 296–301.
23 Y. J. Li, J. Li, S. Ma and Y. J. Luo, *Int. J. Polym. Anal. Charact.*, 2016, **21**, 495–503.
24 Y. Zhao, X. Zhang, W. Zhang, H. J. Xu, W. X. Xie, J. J. Du and Y. Z. Liu, *J. Phys. Chem. A*, 2016, **120**, 765–770.
25 G. Q. Wang, C. X. Zhang, X. H. Guo and Z. Y. Ren, *Spectrochim. Acta, Part A*, 2008, **69**, 407–412.
26 T. R. Hesketh, J. W. C. Van Bogart and S. L. Cooper, *Polym. Eng. Sci.*, 1980, **20**, 190–197.
27 G. Wouter, S. Maria and D. Krijn, *Macromolecules*, 2001, **34**, 1685–1693.
28 A. Jeziorny, *Acta Polym. Sin.*, 1986, **37**, 137–141.